Effects of Visual Stimulation on the Redistribution of Iodine-123-IMP in the Brain Using SPECT Imaging

David A. Weber, Corazon Cabahug, Peter Klieger,* Nora D. Volkow, Christopher Wong, Donald Sacker, and Marija Ivanovic

Nuclear Medicine Research Group, Medical Department, Brookhaven National Laboratory, Upton, New York

A study was performed to validate the assumption that redistribution and clearance of [^{123}I]IMP localization in the brain are unaffected by changes in ambient light levels and visual stimulation occurring after radiopharmaceutical is administered and deposited in the brain. Serial SPECT and planar imaging studies were performed on six healthy, volunteer, adult male subjects under resting, nonactivation conditions. Studies were repeated 7 days later with each subject exposed to strobe light stimulation prior to delayed SPECT procedures at 3 hr. Redistribution and clearance of ^{123}I-IMP in the brain were examined in cortical, subcortical, and cerebellar regions on transaxial slices for the two sets of serial procedures in each subject. Visual stimulation following the initial uptake of [^{123}I]IMP did not affect the distribution or clearance of [^{123}I] IMP in the brain, including the visual cortex, and therefore should not influence the interpretation of delayed SPECT images.

J Nucl Med 1991; 32:1866–1872

The ^{123}I-labeled amine, d,I-N-isopropyl-p-iodoamphetamine hydrochloride (IMP, $C_{12}H_{19}N\ ^{123}IC1$), has been shown to provide a useful radiopharmaceutical to image regional cerebral blood flow (rCBF) (*1–3*). The radiopharmaceutical is sufficiently lipophilic to rapidly diffuse through the blood-brain barrier and its distribution in the brain over the first hour after initial localization is proportional to rCBF. The activity that localizes in the brain is adequate to perform SPECT.

Tomographic images of rCBF within 1 hr after radiopharmaceutical administration have been found extremely useful in the early detection of acute and chronic cerebral infarction, Alzheimer's disease and epileptic foci, and delayed images are used to differentiate peri-infarct ischemia from central necrosis on delayed images (*4–6*). In transitory cerebrovascular events, underperfused regions of the brain seen on early SPECT images may fill in on delayed images (*5,6*). SPECT rCBF studies have been and are being used to assess the effect of pharmacologic, cognitive and sensory stimulation on blood flow in the brain (*7–9*). Concurrent stimulation with radiopharmaceutical administration has been shown to increase rCBF on SPECT imaging studies (*9*). The optimum use of these studies requires that external factors which influence radiopharmaceutical distribution and clearance be known in advance of performing these imaging studies.

Although it is generally assumed that changes in the ambient conditions following the radiopharmaceutical's initial deposition in the brain does not affect localization characteristics, there have been no studies on the effects of external stimulation to validate this assumption. Since visual and auditory stimulation and cognitive mental processes prior to and at the time of radiopharmaceutical administration can lead to changes in the rCBF pattern seen on [^{123}I]IMP SPECT images, this assumption may not be correct. To test the assumption, visual stimulation was performed using a strobe light. Stroboscopic stimulation has been shown to be a good approach for inducing regional brain activation and for increasing rCBF (*10,11*). This investigation provides detailed information on the reproducibility of early cerebral uptake kinetics and distribution characteristics of [^{123}I]IMP on early and delayed SPECT images, and the effects of visual stimulation on the redistribution and retention of previously deposited [^{123}I]IMP.

MATERIALS AND METHODS

Subjects

A group of six volunteer male subjects, ages 27–59, without history of neurologic or psychiatric disease were studied. All subjects received 111 MBq (3 mCi) of [^{123}I]IMP (Iofetamine, Medi-Physics, Inc.) for each of two sets of imaging studies performed seven days apart, with and without visual stimulation. Lugols solution was given to each subject before and after the administration of the radiopharmaceutical to block iodine uptake by the thyroid. The radiopharmaceutical was administered in a quiet and dimly lit room and the subjects were imaged with their eyes open and ears unplugged.

Received Jan. 1, 1991; revision accepted Apr. 3, 1991.

For reprints contact: David A. Weber, PhD, Nuclear Medicine Research Group, Medical Department, Brookhaven National Laboratory, Upton, NY 11973.

* Current address: Department of Radiology, University of Rochester School of Medicine and Dentistry, Rochester, New York.

TABLE 1
Patient Study

Imaging time (min)	Day 0	Day 7	Acquisition parameters			
			View	No. of images	Matrix	Zoom
0– 15	Dynamic planar	Dynamic planar	P-A: head	24– 5 sec	128^2	1.5
				26–30 sec	128^2	1.5
30– 75	SPECT	SPECT	head	60–40 sec	64^2	1.5
165–175	—	Visual stimulation	—	—	—	—
180–225	SPECT	SPECT	head	60–40 sec	64^2	1.5
240–285	SPECT	SPECT	head	60–40 sec	64^2	1.5

Imaging Procedures

All imaging studies were performed using a rotating gamma camera SPECT imaging system (Toshiba GCA-901A) with a 38 × 50.8 cm^2 UFOV. An LEHR collimator was used which provided a measured system spatial resolution of 9.1 mm FWHM at 10 cm depth of scattering material. All images were collected using a 20% energy window, centered on 159.6 keV photopeak of ^{123}I.

Each subject underwent the imaging and associated procedures detailed in Table 1. Serial dynamic images of the brain were recorded in a 128 × 128 pixel matrix and a zoom of 1.5 over the first 15 min (24, 5-sec images and 26, 30-sec images) after radiopharmaceutical administration. Three sets of SPECT images were acquired at 30 min, 3 hr and 4 hr postinjection. SPECT projection data sets were acquired in a step-and-shoot mode using 6° steps over 360° of an elliptical orbit; each projection was acquired for 40 sec. A zoom factor of 1.5 and an acquisition matrix of 64^2 provided a pixel spacing of 5.3 mm. All imaging procedures were conducted with subjects in the supine position. A three-laser beam alignment system was used to position the midline of each patient's head in the center of the acquisition matrix and the canthomeatal line perpendicular to the plane of the detector. With the head immobilized in this position, the plane of the detector was parallel to the coronal plane at 0° and 180° rotation of the detector and parallel to the sagittal plane at 90° and 270° rotation. Static images of two ^{99m}Tc point sources which defined the subject's canthomeatal line was recorded before and after each SPECT acquisition. The influence of visual stim-

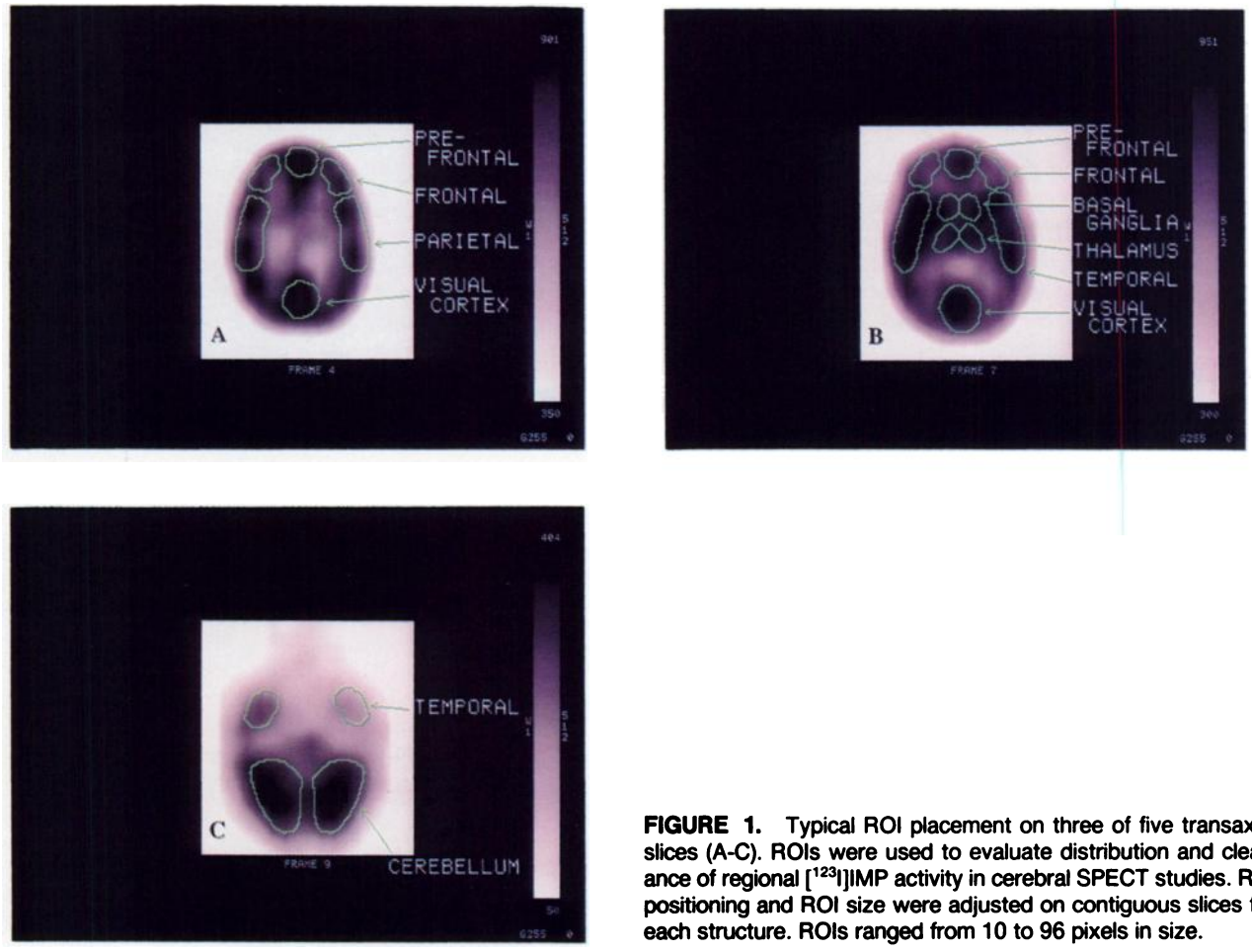

FIGURE 1. Typical ROI placement on three of five transaxial slices (A-C). ROIs were used to evaluate distribution and clearance of regional [^{123}I]IMP activity in cerebral SPECT studies. ROI positioning and ROI size were adjusted on contiguous slices for each structure. ROIs ranged from 10 to 96 pixels in size.

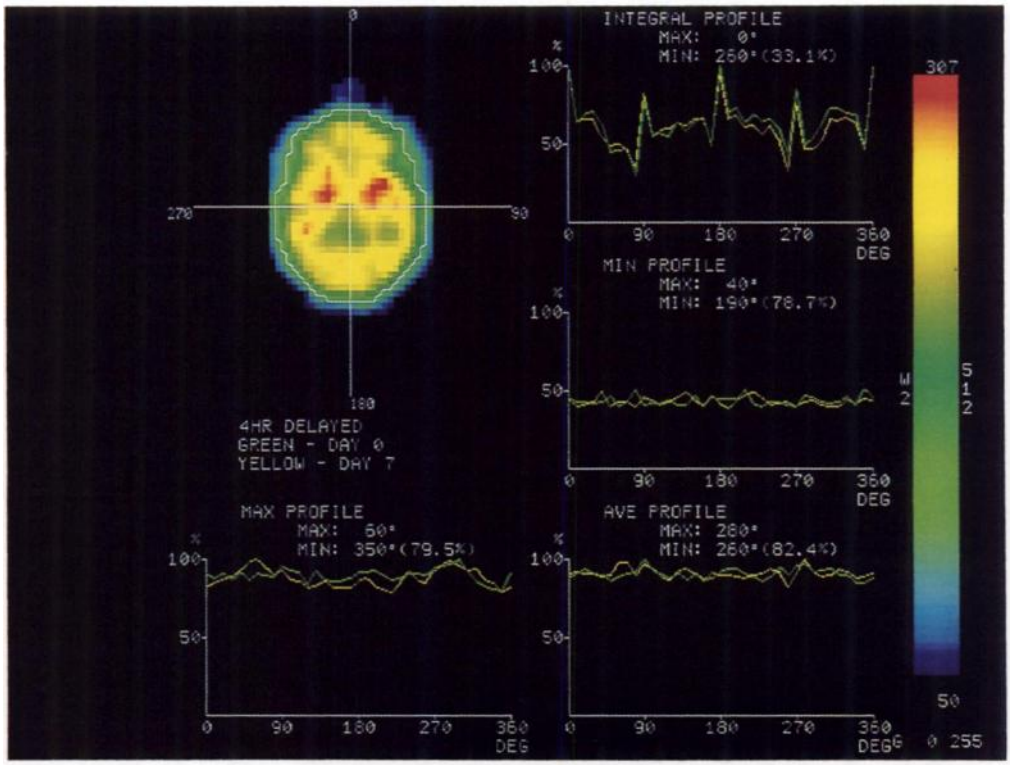

FIGURE 2. Alternative approach to defining ROIs on transaxial brain SPECT images by radial sectoring a single ROI drawn over the cerebral cortex. The cortex for each transaxial slice is subdivided into 36 ROIs, equally spaced at 10-degree increments. ROIs contain 10–25 pixels. The four graphs illustrate the normalized circumferential [^{123}]I-IMP activity profiles of the cortex at the level of the basal ganglia and thalamus for the 4-hr SPECT study performed on Days 0 and 7 in one subject (upper right: total counts/ROI, middle right: minimum counts/pixel/ROI, lower right: average counts/pixel/ROI, lower left: maximum counts/pixel/ROI).

ulation on redistribution of the radiopharmaceutical was tested by exposing each subject to a strobe light between the initial and first of two delayed SPECT imaging studies in the second of the paired studies. Subjects were exposed to a strobe light for 10 min at 165 min following [^{123}I]IMP administration. The strobe light was operated at 11 flashes/sec at an intensity of ~10^6 candela. Subjects were positioned 1.5 meters from the strobe light and were instructed to face the strobe with eyes closed.

Image Processing and Data Analyses

Serial Dynamic Images. A single ROI was placed over both cerebral hemispheres on images collected in the dynamic study to obtain the time-activity curve of [^{123}I]IMP localization in the brain of each subject. Time-activity curves were fit to a dual-exponential function: $y(t) = g - a_1e^{-b_1t} - a_2e^{-b_2t}$. The biologic half-times (T_1 and T_2) and the $T_{50\%}$ and $T_{90\%}$ (the time required for cerebral activity to reach 50% and 90% of the maximum activity observed over the first 15 min) were calculated in each study.

SPECT Studies. Tomographic slices were reconstructed using the filtered backprojection technique with a Shepp-Logan filter. Projections were preprocessed using a uniform high count (120 × 10^6 counts) system flood and a 3 × 3 pixel smoothing filter. Tissue attenuation correction was made by the method described by Chang using an experimentally derived attenuation coefficient of 0.09 cm^{-1} for ^{123}I. Typically, 10–12 transverse tomographic slices of the brain, 2 pixels (10.6 mm) thick, were reconstructed for the region extending from the top of the cortex to the lower edge of the cerebellum, parallel to the orbitomeatal line.

Two different approaches were used to evaluate the distribution characteristics of [^{123}I]IMP. In one, 12 ROIs were identified on five transaxial, 10.6-mm thick, slices to assess the regional activity in the prefrontal, frontal, parietal, temporal, and visual cortex, basal ganglia, and cerebellum (Fig. 1). The ROIs used on each subject were identical in size and shape; only their positioning was changed for different subjects. With the exception of the prefrontal and visual cortex, mirror image ROIs were used to identify contralateral regions for the same structure. ROIs for all regions except the basal ganglia and cerebellum were used to evaluate activity in two adjacent transaxial slices. The activity in the total cortex was taken as the sum of the counts in the cortex for seven or eight contiguous slices. The cortex in each slice was identified by a single ROI defining its external boundary. One set of ROIs was defined for each subject and they were repetitively used to evaluate the six sets of SPECT images obtained in each subject. The redistribution of ^{123}I with and without visual stimulation was evaluated quantitatively from activity ratios of selected regions (as identified by ROIs) to total cortex, contralateral activity ratios in the cortex and basal ganglia, and the regional clearance activity ratios determined from activity ratios of ROIs on the 3-hr and 4-hr SPECT to the 30-min SPECT.

A second approach to evaluating regional brain activity employed a semi-automated radial sectoring of ROIs over the cerebral cortex using an image processing program originally designed for evaluating ^{201}Tl regional myocardial perfusion with circumferential profiles. The cortex was divided into 36 ROIs/slice in equal 10° increments (Fig. 2). The evaluation of the regional activity distribution for serial measurements on the same day or

TABLE 2
Brain Uptake Kinetics

Time	Day 0 n	Day 0 Range (sec)	Day 0 mean ± s.d. (sec)	Day 7 n	Day 7 Range (sec)	Day 7 mean ± s.d. (sec)	p-value*
T_1	5	8– 24	15 ± 6	6	11– 26	17 ± 6	0.081
T_2	5	226–560	392 ± 139	6	260–583	408 ± 153	0.334
$T_{50\%}$	5	40– 80	51 ± 16	6	35– 75	48 ± 18	0.206
$T_{90\%}$	5	585–675	618 ± 34	6	555–680	610 ± 56	0.878

n = no. of subjects.
* t-test for 5 paired values.

repeat measurements on different days are presented as superimposed circumferential profiles.

Statistics

The experimentally determined values of [^{123}I]IMP uptake kinetics and regional localization in the brain are reported as group means ±s.d. or group ranges. The statistical significance of differences in uptake kinetics of [^{123}I]IMP for repeat studies in the same subjects was determined by applying the paired Student's t-test. The same test of significance was applied to the two sets of [^{123}I]IMP localization data obtained with and without visual stimulation. The level of statistical significance was selected at $p < 0.05$.

RESULTS

Since the serial dynamic images and the initial SPECT study are collected prior to the visual stimulation procedure, these data were not influenced by the visual stimulation study and they were used to evaluate the reproducibility of the early phase [^{123}I]IMP uptake and localization in the brain. The time-activity curves derived from the dynamic images were used to characterize the uptake of [^{123}I]IMP in the brain. Table 2 gives the biologic half-times, T_1 and T_2, for the two-component exponential best fit curve of the data and the average times for the activity curve to reach 50% and 90% of the maximum value of the uptake plateau reached within the first 15 min for the six patients in the control/visual stimulation study. The biologic half-times for [^{123}I]IMP uptake in the brain consisted of a fast component with a mean value of 15 sec and 17 sec and a slow component with a mean value of 392 sec and 402 sec for the two consecutive studies on Day 0 and Day 7. Figure 3 shows a typical [^{123}I]IMP cerebral uptake curve fit with a dual-exponential function.

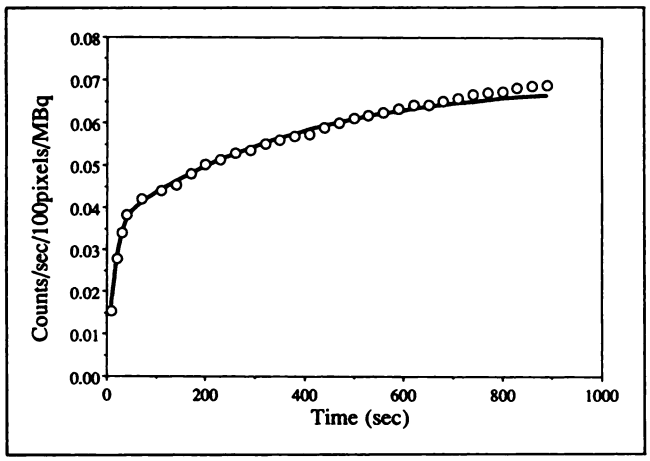

FIGURE 3. An example of a typical biexponential time-activity curve obtained for the uptake of [^{123}I]IMP in the cerebral hemispheres. A single ROI was placed over both cerebral hemispheres on images collected over the first 15 min after injection.

The effects of light stimulation on previously deposited [^{123}I]IMP in the brain was evaluated by comparing the activity distribution in the brain from paired serial SPECT studies collected with (Day 7) and without (Day 0) visual stimulation. All ROI data were obtained using the ROI method shown in Figure 1. The retention of [^{123}I]IMP in different regions of the brain is given in Table 3. The 30-min ROI activity for each structure was assumed to be equal to 1.0 or 100%.

Each retention value is the mean of determinations in six subjects. Retention in the prefrontal, left frontal, parietal and temporal cortex, and basal ganglia ranged from 80% to 84% at 3 hr and 77% to 81% at 4 hr in study 1 performed without visual stimulation. Retention in the same regions in study 2 with visual stimulation ranged from 79% to 81% and 74% to 78%. Retention in the visual cortex and cerebellum were 72% to 73% at 3 hr and 67% to 69% at 4 hr in study 1 and were 72% to 74% at 3 hr and 67% to 73% at 4 hr in study 2.

Regional localization properties of [^{123}I]IMP in the brain are given in Tables 4 and 5. The comparison of regional uptake activity levels to the total cortex in counts/pixel shows the visual cortex to have the highest count density (activity) of all regions on the 30-min SPECT images (Table 4, Fig. 4). Clearing more rapidly than the surrounding tissues and structures, the count density in the visual cortex approaches the levels observed in the cerebellum and temporal and parietal cortex on delayed SPECT. All paired structures including the frontal, temporal, parietal, basal ganglia and cerebellum, gave contralateral uptake

TABLE 3
Iodine-123-IMP Retention

Region	Slice	Retention in transverse slice ROIs*					
		30–70 min		180–220 min		240–280 min	
		C†	VS†	C	VS	C	VS
Prefrontal	S7	1.0	1.0	0.82 ± 0.07	0.81 ± 0.08	0.75 ± 0.07	0.76 ± 0.09
	S6	1.0	1.0	0.82 ± 0.08	0.81 ± 0.06	0.75 ± 0.08	0.74 ± 0.08
L Frontal	S7	1.0	1.0	0.81 ± 0.08	0.79 ± 0.06	0.81 ± 0.09	0.78 ± 0.08
	S6	1.0	1.0	0.82 ± 0.08	0.79 ± 0.05	0.81 ± 0.10	0.77 ± 0.06
L Parietal	S4	1.0	1.0	0.82 ± 0.07	0.81 ± 0.08	0.79 ± 0.09	0.77 ± 0.08
	S3	1.0	1.0	0.82 ± 0.08	0.81 ± 0.06	0.79 ± 0.08	0.77 ± 0.06
L Temporal	S7	1.0	1.0	0.84 ± 0.07	0.82 ± 0.04	0.78 ± 0.09	0.77 ± 0.05
	S6	1.0	1.0	0.82 ± 0.07	0.79 ± 0.05	0.77 ± 0.08	0.75 ± 0.04
Visual	S4	1.0	1.0	0.72 ± 0.09	0.72 ± 0.04	0.69 ± 0.08	0.73 ± 0.07
	S3	1.0	1.0	0.73 ± 0.07	0.74 ± 0.05	0.69 ± 0.07	0.67 ± 0.04
L Basal ganglia	S6	1.0	1.0	0.80 ± 0.11	0.80 ± 0.06	0.77 ± 0.11	0.76 ± 0.07
Cerebellum	S8	1.0	1.0	0.72 ± 0.06	0.72 ± 0.05	0.67 ± 0.07	0.67 ± 0.05

* Retention expressed as mean value in six subjects ± s.d.
† Control study (C) on Day 0; visual stimulation (VS) at 165 min on Day 7.

TABLE 4
Activity Ratio of Region-to-Total Cortex*

Region	Slice	Transverse slice image ROIs					
		30–70 min		180–220 min		240–280 min	
		C†	VS†	C	VS	C	VS
Prefrontal	S7	1.04 ± 0.04	1.04 ± 0.04	1.04 ± 0.07	1.05 ± 0.03	1.05 ± 0.05	1.07 ± 0.07
	S6	1.07 ± 0.06	1.06 ± 0.06	1.05 ± 0.09	1.07 ± 0.04	1.07 ± 0.05	1.07 ± 0.07
L Frontal	S7	0.94 ± 0.04	1.06 ± 0.05	0.95 ± 0.09	0.98 ± 0.07	1.02 ± 0.06	1.02 ± 0.09
	S6	1.00 ± 0.03	1.12 ± 0.02	1.02 ± 0.09	1.04 ± 0.03	1.09 ± 0.04	1.06 ± 0.04
L Parietal	S4	1.06 ± 0.03	1.08 ± 0.04	1.09 ± 0.07	1.14 ± 0.03	1.13 ± 0.04	1.14 ± 0.05
	S3	1.06 ± 0.03	1.07 ± 0.03	1.08 ± 0.08	1.12 ± 0.04	1.12 ± 0.02	1.12 ± 0.03
L Temporal	S7	1.03 ± 0.06	1.06 ± 0.05	1.10 ± 0.08	1.13 ± 0.05	1.10 ± 0.05	1.11 ± 0.06
	S6	1.09 ± 0.04	1.12 ± 0.02	1.12 ± 0.09	1.13 ± 0.04	1.12 ± 0.05	1.14 ± 0.04
Visual	S4	1.23 ± 0.04	1.25 ± 0.06	1.13 ± 0.04	1.14 ± 0.04	1.14 ± 0.03	1.13 ± 0.03
	S3	1.22 ± 0.03	1.23 ± 0.04	1.10 ± 0.10	1.17 ± 0.02	1.14 ± 0.03	1.15 ± 0.04
L Basal ganglia	S6	1.04 ± 0.05	1.05 ± 0.04	1.03 ± 0.08	1.09 ± 0.07	1.07 ± 0.06	1.09 ± 0.05
Cerebellum	S8	1.07 ± 0.04	1.08 ± 0.04	1.12 ± 0.10	1.18 ± 0.03	1.15 ± 0.04	1.15 ± 0.05

* Activity in counts/pixel, ratios expressed as mean value in six subjects ± s.d.
† Control study (C) on Day 0; visual stimulation study (VS) on Day 7.

TABLE 5
Contralateral Uptake Ratios from SPECT Images

Region	Slice	n	30–70 min		180–220 min		240–280 min	
			C*	VS*	C	VS	C	VS
Frontal	S7	6	0.97 ± 0.03	0.98 ± 0.05	1.01 ± 0.07	0.99 ± 0.04	1.03 ± 0.09	1.00 ± 0.05
	S6	6	0.99 ± 0.02	1.00 ± 0.04	1.01 ± 0.05	1.00 ± 0.04	1.04 ± 0.06	1.00 ± 0.06
Temporal	S7	6	0.97 ± 0.04	0.97 ± 0.05	1.01 ± 0.05	1.00 ± 0.05	0.98 ± 0.06	0.99 ± 0.05
	S6	6	0.96 ± 0.04	0.98 ± 0.03	1.01 ± 0.03	1.00 ± 0.02	0.99 ± 0.03	1.00 ± 0.05
Basal ganglia	S6	6	1.01 ± 0.04	1.01 ± 0.04	0.98 ± 0.06	0.99 ± 0.05	0.96 ± 0.04	0.96 ± 0.05
Parietal	S3	6	0.97 ± 0.04	0.99 ± 0.04	1.02 ± 0.05	1.02 ± 0.04	1.02 ± 0.04	1.00 ± 0.06
	S3	6	0.98 ± 0.04	0.99 ± 0.02	1.03 ± 0.04	1.04 ± 0.04	1.04 ± 0.02	1.01 ± 0.04
Cerebellum	S9	6	0.99 ± 0.05	0.97 ± 0.05	0.98 ± 0.03	0.94 ± 0.03	0.94 ± 0.03	0.96 ± 0.03
	S8	6	0.99 ± 0.05	1.00 ± 0.04	1.00 ± 0.02	0.98 ± 0.02	0.99 ± 0.05	0.99 ± 0.02

* n = No. of subjects.
** Ratio expressed as mean value in 6 subjects ± s.d.

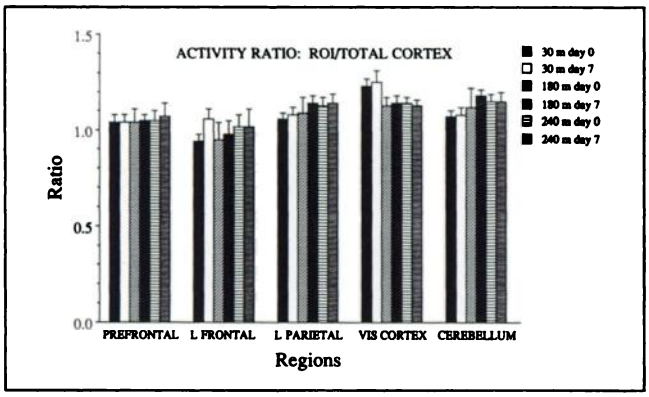

FIGURE 4. Graph showing comparison of the ratios of regional uptake to total cortex activity indicate that localization and clearance properties of [^{123}I]IMP in cortical, subcortical and cerebellar regions of the brain are not influenced by visual stimulation occurring after [^{123}I]IMP localization.

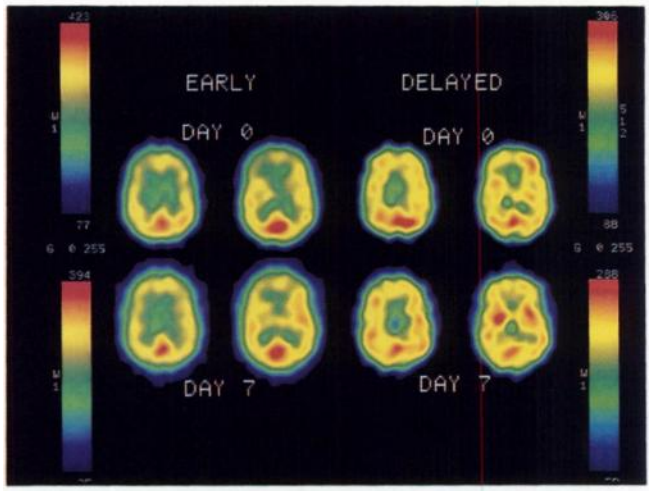

FIGURE 5. Paired image set: Two transaxial slices taken at 30 min and 4 hr on Day 0 (control) and Day 7 (visual stimulation) demonstrate reproducibility of [^{123}I]IMP localization at the level of the mid-brain. Upper row: two images on left are contiguous 10.6-mm thick slices acquired at 30 min after injection on Day 0; two images on right are the same slices at 4 hr after injection. Lower row: the same combination of transaxial slices recorded on Day 7.

ratios that randomly varied about 1.0 (Table 5), ranging from 0.96 to 1.04 in both studies (Days 0 and 7).

DISCUSSION

The activity distribution of [^{123}I]IMP in the brain is a relatively complex function of the lipophilic properties, charge, and molecular weight of the radiopharmaceutical, blood flow to and rCBF within the brain, the availability of "nonspecific" receptor sites for the labeled amine, the metabolism of [^{123}I]IMP (initial dealkylation of the IMP to p-iodoamphetamine), pH, permeability of cerebral structures, release of [^{123}I]IMP from the lungs, as well as several other factors (*12–15*). It is assumed that any redistribution or changes in the rCBF distribution pattern, established during the first hour following [^{123}I]IMP administration, will not be influenced by changes in ambient room conditions that occur at later times. Redistribution and changes in tracer clearance seen on delayed images reflect the patient's condition and the chemical behavior of the tracer in vivo. The importance of delayed imaging to evaluate some types of cerebrovascular disease makes it necessary to rule out external factors that could easily occur during the waiting period between procedures and that might influence the redistribution or clearance of the radiopharmaceutical seen on delayed images. The reproducibility of the uptake kinetics and rCBF distribution pattern were tested here under identical conditions over the first 70 min after radiopharmaceutical administration. The effects of visual stimulation at 165 min after radiopharmaceutical administration were evaluated by quantitatively comparing delayed SPECT images at 3 and 4 hr in the same subject with and without visual stimulation.

The cerebral uptake kinetics defined by T_1, T_2, $T_{50\%}$, and $T_{90\%}$ showed the rates of [^{123}I]IMP deposition to be highly variable among subjects, but reproducible in the same subject (Table 2). Despite a variation of more than a factor of two in uptake half-times among the subjects, e.g., on Day 0, T_2 = 226–560 sec (n = 5) and on Day 7, T_2 = 260–583 sec (n = 6), paired studies in the same subject showed reproducible rates of uptake. Repeated assays of T_1 and T_2 yielded mean values of 15 ± 6 sec and 392 ± 139 sec on Day 0 and 17 ± 6 sec and 408 ± 153 sec on Day 7, respectively. Comparison of the average half-times calculated from the time-activity curves in study one and study two for the five subjects having two studies gave p-values of 0.081 for T_1 and 0.334 for T_2. A similar close correlation was observed for $T_{50\%}$ and $T_{90\%}$: 51 ± 16 sec and 618 ± 34 sec on Day 0 and 48 ± 18 sec and 610 ± 56 sec on Day 7.

Visual inspection of the regional deposition of [^{123}I]IMP on early and delayed SPECT images between the control study on Day 0 and the visual stimulation study on Day 7 showed minor variations in uptake, however, no focal or significant differences in the distribution of the radiopharmaceutical. An example of the paired image sets are shown in Figure 5. The serial SPECT studies performed at 30 min, 3 hr and 4 hr showed a slowly decreasing [^{123}I] IMP uptake ratio between gray and white matter similar to what has been reported previously (*3,4,16*). Otherwise no significant changes in radiopharmaceutical distribution were seen between the control and visual stimulation studies in the normal control subjects. To confirm these impressions and to evaluate quantitatively the relative distribution and clearance characteristics with and without visual stimulation, the set of ROIs developed for each subject (Fig. 1) were used to evaluate distribution properties of the radiopharmaceutical in six sets of SPECT images collected in the control and visual stimulation studies. The data presented in Tables 3, 4, and 5 summarize the quan-

titative results. The activity profiles obtained with the finer spaced, radially selected ROIs (Fig. 2) provide a useful means of monitoring regional activity throughout the entire cortex seen in each slice; this was used to look for trends and variations in regional perfusion that extended beyond the discretely flagged ROIs in serial images or for images collected on separate days. This is similar to the approach used by Maurer et al. (*17*) to evaluate cerebral perfusion before and after carotid endarterectomy.

Comparison of regional clearance in selected ROIs over the prefrontal, left frontal, left parietal, left temporal, and visual cortex, left basal ganglia, and cerebellum show no significant differences in clearance between the control and the visual stimulation study (Table 3, Fig. 4). Three- and 4-hr retention values for the different regions randomly vary by 1%–2% in 43 of 48 determinations of retention in 12 ROIs examined at 3 and 4 hr on the control and visual stimulation studies. Paired t-test p values ranged from 0.243 to 0.928. The results showed [^{123}I]IMP to clear the visual cortex and cerebellum significantly faster than the remaining regions of the cortex and basal ganglia. The greater clearance seen in the cerebellum resembles other observations in the literature (*4,5*), however, retention in all structures was significantly less than that reported by Nishizawa et al. (*4*) and significantly greater than that reported by Creutzig et al. (*5*).

Activity ratios of all ROIs compared to total cortex (Table 4), contralateral activity ratios of paired left and right structures (Table 5), and activity profiles (Fig. 2) were consistent with the retention measurements. Delayed visual stimulation did not affect activity distributions seen on delayed SPECT. With the exception of a single value for one ROI, paired t-test p values showed no significant differences between the distribution characteristics of [^{123}I] IMP on delayed views with or without visual stimulation. The p values ranged from 0.154 to 0.998. The visual cortex showed the highest concentration of activity on the initial rCBF images at 30 min and the visual cortex, temporal and parietal cortex structures showed the highest activity on delayed images at 180 min and 240 min. The contralateral ratios for paired studies seen in Table 5 showed random variation about 1.0 and symmetrical uptake was maintained in all paired structures on early and delayed images.

CONCLUSION

A qualitative and quantitative evaluation of serial [^{123}I] IMP SPECT imaging studies conducted 7 days apart in control subjects showed that [^{123}I]IMP localization and clearance is reproducible in subjects without history of neurologic or psychiatric disease. A similar close correlation was observed for repeat studies of [^{123}I]IMP cerebral uptake kinetics over the first 30 min following radiopharmaceutical administration. Strobe light visual stimulation did not influence the regional distribution or clearance of deposited [^{123}I]IMP. These findings indicate that visual stimulation occurring after [^{123}I]IMP deposition will not affect the redistribution of [^{123}I]IMP on delayed SPECT images and, therefore, should not influence interpretation of these images.

ACKNOWLEDGMENT

Research supported by U.S. DOE contract DE-AC02-76CH00016.

REFERENCES

1. Kuhl DE, Barrio JR, Huang S-C, et al. Quantifying local cerebral blood flow by N-isopropyl-p-[^{123}I]iodoamphetamine (IMP) tomography. *J Nucl Med* 1982;23:196–203.
2. B. L. Holman, ed. *Radionuclide imaging of the brain.* New York: Churchill Livingstone; 1985.
3. Holman BL, Tumeh SS. Single-photon emission computed tomography. *JAMA* 1990;263:561–564.
4. Nishizawa S, Tanada S, Yonekura, Y, et al. Regional dynamics of N-isopropyl-(^{123}I)p-iodoamphetamine in human brain. *J Nucl Med* 1989;30:150–156.
5. Creutzig H, Schober O, Gielow P, et al. Cerebral dynamics of N-isopropyl(^{123}I)p-iodoamphetamine. *J Nucl Med* 1986;27:178–183.
6. Defer G, Moretti J-L, Cesaro P, Sergent A, Raynaud C, Degos J-D. Early and delayed SPECT using N-isopropyl-p-iodoamphetamine iodine-123 in cerebral ischemia. *Arch Neurol* 1987;44:715–718.
7. Weber DA, Klieger P, Volkow ND, et al. SPECT regional cerebral blood flow (rCBF) studies in crack users and control subjects [Abstract]. *J Nucl Med* 1990;31:876.
8. Tumeh SS, Nagel JS, English RJ, et al. Cerebral abnormalities in cocaine abusers: demonstration by SPECT perfusion brain scintigraphy. *Radiology* 1990;176:821–824.
9. Woods SW, Hegeman IM, Zubal IG, et al. Visual stimulation increases technetium-99m-HMPAO distribution in human visual cortex. *J Nucl Med* 1991;32:210–215.
10. Celesia G, Polcyn RD, Holden JE, et al. Visual evoked potentials and positron emission tomographic mapping of regional cerebral blood flow and cerebral metabolism. *Electroenceph and Clin Neurophys* 1982;54:243–256.
11. Volkow ND, Mullani N, Gould L, Gatley SJ. Sensitivity of measurements of regional brain activation with ^{15}O-water and PET to time of stimulation and period of image reconstruction. *J Nucl Med* 1991:in press.
12. Winchell HS, Baldwin RM, Lin TH. Development of I-123-labeled amines for brain studies: localization of I-123-iodophenylalkyl amines in rat brain. *J Nucl Med* 1980;21:940–946.
13. Baldwin RM, Wu J-L. In vivo chemistry of iofetamine HCl iodine-123 (IMP). *J Nucl Med* 1988;29:122–124.
14. Baldwin RM, Lin T-H, Wu J-L, Lamb JF. Receptors for amphetamines. In: Biersack HJ, Winkler C, eds. *Amphetamines and pH-shift agents for brain imaging, basic research and clinical results.* Berlin: Walter de Gruyter; 1986:19–23.
15. Biselof-Delaloye A, Delaloye B. Biokinetics of N-isopropyl-p-[I-123]iodoamphetamine in the human. In: Biersack HJ, Winkler C, eds. *Amphetamines and pH-shift agents for brain imaging, basic research and clinical results.* Berlin: Walter de Gruyter; 1986:45–50.
16. Nakano S, Kinoshita K, Jinnouchi S, Hoshi H, Watanabe K. Critical cerebral blood flow thresholds studied by SPECT using xenon-133 and iodine-123-iodoamphetamine. *J Nucl Med* 1989;30:337–342.
17. Maurer AH, Siegel JA, Comerota AJ, et al. SPECT quantification of cerebral ischemia before and after carotid endarterectomy. *J Nucl Med* 1990;31:1412–1420.